

LA-UR- 98-2608

*Approved for public release;
distribution is unlimited.*

Title:

Structural and Magnetic Characterization
of Actinide Materials

Author(s):

Barbara Cort, Luis Morales,
 John M. Haschke, Paul W. Watson III,
 Paul G. Klemens, NMT-11 MAT
 Thomas H. Allen, Fidel A. Vigil, NMT-5,
 Andrew C. Lawson, MST-8
 Juergen Eckert, LANSCE-12

Peter Vorderwisch
 Hahn-Meitner Institute, Berlin

Submitted to:

DOE OFFICE OF SCIENTIFIC AND TECHNICAL
INFORMATION (OSTI)

RECEIVED
 DEC 21 1998
 OSTI

UNCLASSIFIED NOT UCNI

PL JUN 15 1998
 date

S-7

MASTER

DISTRIBUTION OF THIS DOCUMENT IS UNLIMITED

Los Alamos

NATIONAL LABORATORY

Los Alamos National Laboratory, an affirmative action/equal opportunity employer, is operated by the University of California for the U.S. Department of Energy under contract W-7405-ENG-36. By acceptance of this article, the publisher recognizes that the U.S. Government retains a nonexclusive, royalty-free license to publish or reproduce the published form of this contribution, or to allow others to do so, for U.S. Government purposes. Los Alamos National Laboratory requests that the publisher identify this article as work performed under the auspices of the U.S. Department of Energy. The Los Alamos National Laboratory strongly supports academic freedom and a researcher's right to publish; as an institution, however, the Laboratory does not endorse the viewpoint of a publication or guarantee its technical correctness.

DISCLAIMER

This report was prepared as an account of work sponsored by an agency of the United States Government. Neither the United States Government nor any agency thereof, nor any of their employees, makes any warranty, express or implied, or assumes any legal liability or responsibility for the accuracy, completeness, or usefulness of any information, apparatus, product, or process disclosed, or represents that its use would not infringe privately owned rights. Reference herein to any specific commercial product, process, or service by trade name, trademark, manufacturer, or otherwise does not necessarily constitute or imply its endorsement, recommendation, or favoring by the United States Government or any agency thereof. The views and opinions of authors expressed herein do not necessarily state or reflect those of the United States Government or any agency thereof.

DISCLAIMER

**Portions of this document may be illegible
in electronic image products. Images are
produced from the best available original
document.**

Structural and Magnetic Characterization of Actinide Materials

Barbara Cort,* Thomas H. Allen, Andrew C. Lawson, Luis Morales, John M. Haschke,
Paul W. Watson, III, Paul G. Klemens, Juergen Eckert, and Fidel A. Vigil
Los Alamos National Laboratory

Peter Vorderwisch
Hahn-Meitner Institute, Berlin

Abstract

This is the final report of a three-year, Laboratory Directed Research and Development (LDRD) project at Los Alamos National Laboratory (LANL). We have successfully used neutron scattering techniques to investigate physicochemical properties of elements, compounds, and alloys of the light actinides. The focus of this work is to extend our fundamental research capability and to address questions of practical importance to stockpile integrity and long-term storage of nuclear material. Specific subject areas are developing neutron diffraction techniques for smaller actinide samples; modeling of inelastic scattering data for actinide metal hydrides; characterizing actinide oxide structures; and investigating aging effects in actinides. These studies utilize neutron scattering supported by equilibrium studies, kinetics, and x-ray diffraction. Major accomplishments include (1) development of encapsulation techniques for small actinide samples and neutron diffraction studies of $\text{AmD}_{2.4}$ and $\text{PuO}_{2.3}$; (2) refinement of lattice dynamics model to elucidate hydrogen-hydrogen and hydrogen-metal interactions in rare-earth and actinide hydrides; (3) kinetic studies with PuO_2 indicating that the recombination reaction is faster than radiolytic decomposition of adsorbed water but a chemical reaction produces H_2 ; (4) PVT studies of the reaction between PuO_2 and water demonstrate that PuO_{2+x} and H_2 form and that PuO_2 is not the thermodynamically stable form of the oxide in air; and (5) model calculations of helium ingrowth in aged plutonium predicting bubble formation only at grain boundaries at room temperature. The work performed in this project has application to fundamental properties of actinides, aging, and long-term storage of plutonium.

Background and Research Objectives

We have studied temperature-dependent physicochemical properties of actinide metals, alloys and compounds using PVT and kinetic measurements, electrical resistivity, thermal expansion, and neutron scattering techniques in support of the weapons program for many years. The focus of this LDRD project was to extend our fundamental research

* Principal Investigator, e-mail address: bcort@lanl.gov

capability to address questions of practical importance to stockpile integrity and long-term storage of nuclear material. Specific objectives were (1) extension of neutron diffraction techniques to study smaller samples of actinide materials, (2) modeling of neutron inelastic scattering data, (3) studies of plutonium oxides under long-term storage conditions, and (4) preliminary studies of aging effects in plutonium.

During this project, we developed encapsulation techniques for milligram quantities of actinides for neutron scattering studies and used the encapsulation to perform structural studies of $\text{AmD}_{2.4}$ and PuO_{2+x} . We investigated the interaction of H_2 and O_2 with PuO_2 and the interaction of water with PuO_2 under storage conditions. We developed a preliminary model for neutron inelastic scattering data of rare earth hydrides. We also used elasticity theory to calculate thermodynamic properties of helium in aged plutonium.

Importance to LANL's Science and Technology Base and National R&D Needs

Actinide research has historically been an integral part of the Laboratory's mission. An understanding of the fundamental properties of actinides is essential to our goals as stewards of the enduring stockpile. A complete picture of actinide behavior requires data for all members of the actinide series and modeling techniques to compliment experiment. Our studies of actinide metals, compounds, and alloys have thus far been limited to those elements, primarily plutonium and neptunium isotopes, that are available in gram quantities. However, a physical picture of actinide behavior is incomplete without data for those actinide elements available only in milligram quantities or that are difficult to handle in gram quantities due to radiological properties. A specific example is americium, which grows in ^{239}Pu as a result of the decay of the ^{241}Pu isotopic contaminant.

Neutron scattering techniques are powerful for the study of actinides because as a bulk probe, they are very effective in characterizing reactive and structurally and behaviorally complex materials. Extension of our neutron scattering techniques, both experimental and theoretical, enhances the value of these tools. The development of both small sample encapsulation methods and enhanced modeling techniques for these data fulfill basic needs for actinide research.

Long-term storage of nuclear materials has recently emerged as a challenging problem that requires studied solutions. Clearly, the solution of problems related to long-term storage of nuclear materials has applicability throughout the DOE complex. It is expected that the lifetime of a weapon in stockpile will increase and it is not known how nuclear materials aging will affect performance. Because underground testing is not available to test performance of aged and aging pits in the enduring stockpile, effects must

be determined indirectly by measuring material properties and how they change with age. One phenomenon that has been identified as a potential problem is the accumulation of helium as a product of radioactive decay in aged plutonium. Further, because plutonium stored in air oxidizes easily, the stability of plutonium oxides under long-term storage conditions is an issue of concern.

Scientific Approach and Accomplishments

I. *Structural Studies of AmD_x* (Tom Allen, John Haschke, and Paul Watson, NMT-5; A. C. Lawson, MST-5)

We successfully used welded, thin-walled vanadium containers to doubly encapsulate actinide samples, both powders and solid metal samples, with masses in the range 10-30 g. To study milligram quantities of actinides, new encapsulation techniques are required to allow even further reduction of the neutron scattering signal from the encapsulation material. We modified our basic design by reducing the overall size of the assembly and by resting the inner capsule on a thin-walled vanadium standoff to lift the sample off the thick vanadium bottom, thereby reducing the amount of vanadium in the neutron beam (Figure 1).

In FY 1996, we performed a successful test on a non-radioactive sample using the new encapsulation assembly. We observed clear diffraction peaks (Figure 2) for 15 mg of CaF₂ counting for two hours on the Manuel Lujan Neutron Scattering Center (MLNSC) High-Intensity Powder Diffractometer (HIPD). We used these results to calculate patterns for two actinides of interest, AmD₂ and PuO₂, each counted for 24 hours (Figure 2); the model predicted well-defined diffraction peaks. In FY 1997, we performed a neutron diffraction study of the structural properties of a 200-mg sample of ²⁴³AmD_{2.4} using the new encapsulation assembly and the same instrument. This arrangement worked even better than expected, and a room temperature diffraction pattern after about 6 hours of beam is shown in Figure 3.

It was anticipated that the crystal structure of this material would be a superstructure of the cubic fluorite structure, and the best solution we have found so far is a tetragonal structure with twice the fluorite volume. However, it was not possible to obtain an unambiguous determination of the crystal structure, because numerous small peaks are not indexed, and we do not know whether these are super-lattice peaks of an even larger structure or signs of impurity phases. The structure found here is different from that found for NpD_{2.1}, as the basal plane area is doubled for the AmD_{2.4} structure, while the c-axis

length is doubled for the $\text{NpD}_{2.1}$ structure. The tetrahedral occupancy is 1.9, and the octahedral occupancy is 0.5. Atomic positions for our model are given in Table 1. We

Table 1. Crystal data for $\text{AmD}_{2.4}$ at 300K. Space group is P4/mmm with lattice parameters $a = 7.490 \text{ \AA}$, $c = 5.352 \text{ \AA}$.

atom	x	y	z	frac
Am(1)	0	0	0	1
Am(2)	-	-	0	1
Am(3)	.261	.261	-	1
Am(4)	-	0	0	1
D(5)	0	0	-	0
D(6)	-	-	-	.98
D(7)	.225	.225	0	.70
D(8)	-	0	0	0
D(9)	.233	0	.259	1.06
D(10)	-	.233	.220	.80

investigated the structure at different temperatures and found that the lattice constants vary in a normal way (Figure 4). The deuterium occupancies are not significantly temperature dependent, and no structural correlates were found for the reported anomalies in the electrical resistivity[1]. However, the true structure may be more complicated than reported here.

2. *Modeling of Inelastic Neutron Scattering Data for Rare-Earth and Actinide Hydrides* (Paul Watson, NMT-5; Juergen Eckert, MLNSC; Peter Vorderwisch, Hahn-Meitner Institute, Berlin)

We used a lattice dynamics model to calculate the phonon density of states for comparison with inelastic neutron scattering data for cubic rare-earth and actinide hydrides in order to describe metal-hydrogen and hydrogen-hydrogen interactions in these systems. We use CeH_x with the BiF_3 structure as a well-characterized simple prototype and choose a dynamic supercell of size $2a \times 2a \times 2a$, where a is the lattice parameter. For stoichiometric CeH_3 , there is then a total of $N=128$ atoms: 32 Ce atoms, 64 H_t atoms on tetrahedral sites, and 32 H_o atoms on octahedral sites. The non-stoichiometric hydride is simulated by removing hydrogen atoms from the octahedral sites. For simplicity, we have thus far performed the calculation only for zero wave vector ($q = 0$). The steps in the calculation are as follows: (1) Born-von Kármán tensor force models describe the interaction between each type of atom out to second nearest-neighbor atoms. The crystal symmetries are used to reduce the number of variable parameters. (2) The dynamic matrix is diagonalized to

determine the eigenfrequencies. (3) The frequencies are divided into intervals, and the number of frequencies in each interval is determined, giving a histogram. (4) The histogram is convoluted with a gaussian distribution to get a representation of the phonon density of states. The resulting spectrum for $\text{CeH}_{2.09}$ with $q=0$ shows peaks in the correct positions, but not all have the correct intensity (Figure 5). This problem can be corrected by extending the calculation to $q>0$.

3. *Characterization of the Reactions of PuO_2 with Water* (Thomas H. Allen, John M. Haschke, Charles L. Radosevich, and Luis Morales, NMT-5)

Due to the reduction in the number of nuclear weapons, the storage of surplus weapons-related nuclear material is an important issue. A large body of data related to the long-term storage of plutonium metal exists because of extensive experience gained from storing metal in weapons components. However, the consequences of extended storage of secondary materials such as plutonium dioxide (PuO_2) are inadequately understood. In part, this lack of information has not previously been a concern because the oxide was rapidly reprocessed to metal for weapon fabrication. Since oxide must be stored in sealed containers, a critical issue is the amount of water (H_2O) remaining on oxide placed in storage. It is possible that radiolytic decomposition of the residual water, while the oxide is in a sealed container, would result in gas pressures large enough to rupture the container. There are three possible reactions: (1) Adsorbed water radiolytically decomposes to hydrogen (H_2) and oxygen (O_2), resulting in a pressure increase in the container. (2) Adsorbed water chemically reacts with the oxide, releasing H_2 gas, while oxygen forms a higher-stoichiometry oxide. In this case, the calculated pressure rise is only 67% of that in case (1). (3) H_2 and O_2 gases recombine on the catalytic oxide surface to form H_2O . The second reaction opposes radiolytic decomposition and, based on the rates of the two opposing processes (decomposition and recombination), an equilibrium pressure should be established in the container.

To gain insight into the $\text{PuO}_2/\text{H}_2\text{O}$ system, we conducted experiments to investigate the interaction of H_2 and O_2 with PuO_2 and the interaction of water with PuO_2 . We collected pressure and temperature data as a function of time for ten-gram samples of PuO_2 exposed to two different storage conditions. In one reactor, we added stoichiometric quantities of deuterium (D_2) and oxygen (O_2) gases. In another reactor, we saturated the PuO_2 with deuterium oxide (D_2O) at its room-temperature vapor pressure. Periodically, we removed aliquots of gas from each reactor for analysis. Results show that the rate of combination of D_2 and O_2 on the catalytic surface of the oxide is much faster than the rate of dissociation of D_2O (Figure 6). In addition, results of gas analysis from the water vapor

experiment suggest that an observed pressure increase (13 nmol D₂/g d) results from formation of a higher plutonium oxide rather than by radiolytic decomposition of water.

We conducted neutron diffraction studies to determine the structures of the oxide reaction product. We synthesized hyper-stoichiometric oxide, ²⁴²PuO_{2+x}, by reacting 400 mg of the ²⁴²PuO₂ starting material with water vapor. We carried out the reaction in the pressure-volume-temperature (PVT) apparatus under the following conditions. We fixed the temperature of the oxide ²⁴²PuO₂ at 300°C under a dynamic vacuum for eight hours in order to remove adsorbed surface species. We introduced water vapor, at a fixed pressure of 18 Torr, into the reaction chamber from a thermostatic water reservoir. We maintained the oxide ²⁴²PuO₂ at a temperature of 300°C and allowed it to react with the water vapor for approximately 30 days. After that time, we removed the oxide product ²⁴²PuO_{2+x} from the PVT apparatus and encapsulated it in vanadium for neutron powder diffraction. We ran the sample of PuO_{2+x} on the HIPD for a period of about 1 day. Unfortunately, the sample turned out to be much smaller than originally planned, but this was not known in time to use the small sample holders designed for AmD_{2.4}. As a result, the background from the vanadium is quite high. Some of the background may be incoherent scattering from the hydrogenous water known to be present in the sample. A diffraction pattern is shown in Figure 7, with peaks from both vanadium and from PuO₂. We used a simple fluorite structure model for PuO₂. The refined stoichiometry is PuO_{2.30(8)}, and the lattice constant is 5.395 Å.

4. *Aging Effects in Plutonium* (Paul G. Klemens, University of Connecticut)

One problem of importance to our aging stockpile is the formation of helium bubbles in aged plutonium. A natural product of isotopic decay in plutonium is helium gas that accumulates over time. Helium bubbles have been discovered in aged plutonium samples subjected to various heat treatments using transmission electron microscopy[2]. It is not understood how the trapped helium will affect material performance and properties in nuclear weapons. We used elasticity theory to calculate the gas pressure inside a helium bubble generated in a plutonium matrix. The results predict that a gas bubble expands by plastic yield until the pressure inside is approximately $\frac{2}{3}$ the yield stress. Additionally, our calculation of the chemical potential of a gas atom inside the bubble implies that bubbles can form only at grain boundaries at room temperature.

Publications

1. Haschke, J. M., and Ricketts, T. E., "Adsorption of water on Plutonium oxide," *J. Alloys Compounds*, **252**, 148-156 (1997).
2. Klemens, P. G. and Cort, B., "Thermodynamic properties of helium bubbles in aged plutonium," *J. Alloys and Compounds*, **252**, 157-161 (1997).
3. Haschke, J. M., T. H. Allen, and J. L. Stakebake, "Reaction kinetics of plutonium with oxygen, water, and humid air," *J. Alloys Compounds*, **243**, 23-35, (1996).

References

- [1] Cort, B., Ward, J. W., Vigil, F. A. , and Haire, R. G., "Resistivity studies of cubic americium hydrides from 20 to 300 K," *J. Alloys and Compounds*, **224**, 237-240 (1997).
- [2] Zocco, T. G., and Rohr, D. L., "Developments in the TEM Examination of Pu and Pu Alloys," *Mater. Res. Soc. Proc.*, **115**, 259, (1988).

ASSEMBLY: SMALL VANADIUM SAMPLE HOLDER

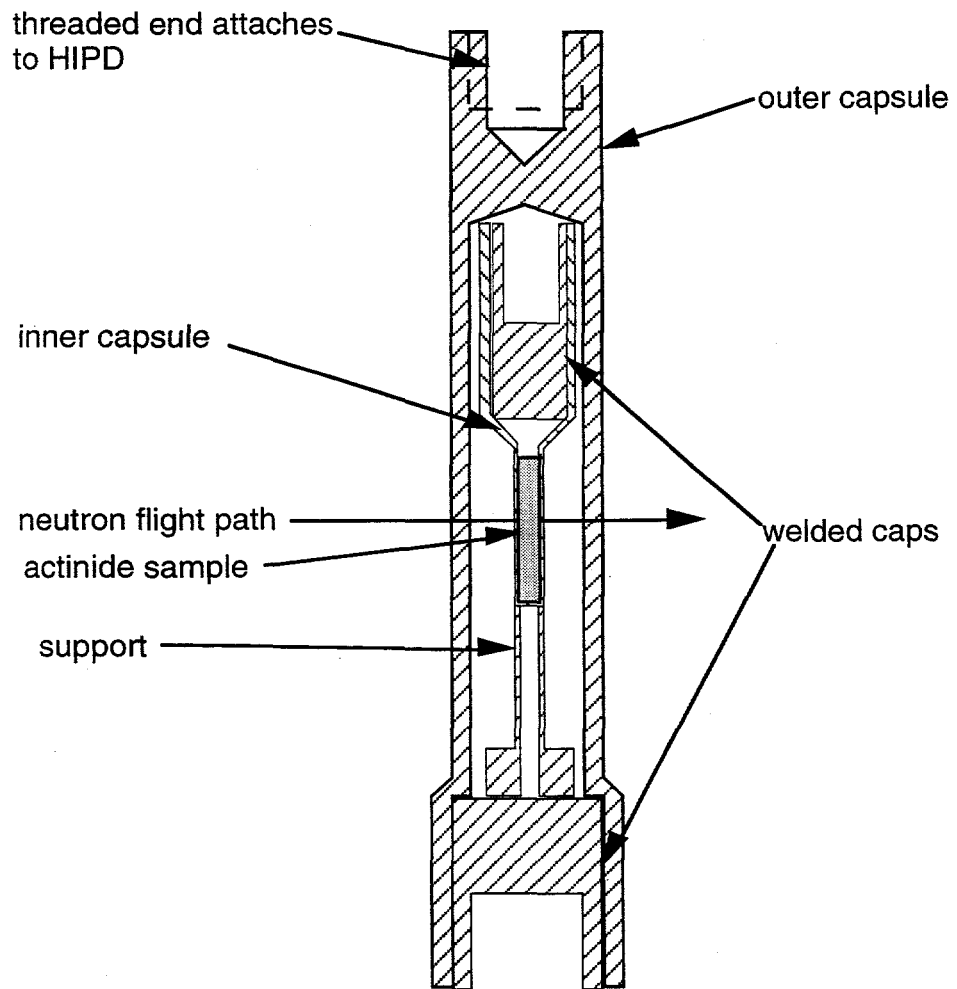
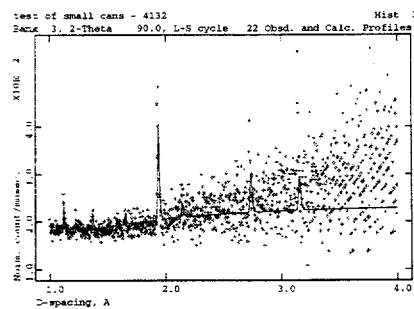
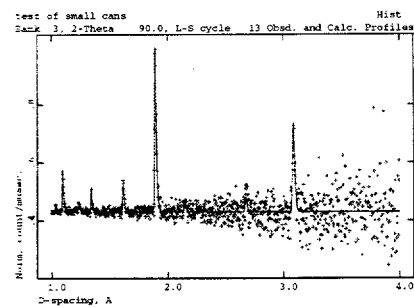
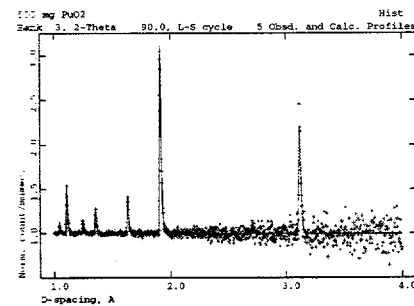


Figure 1. Vanadium encapsulation assembly for mg-sized samples of actinides.

15 mg. CaF_2 - 2 hours - measured100 mg. AmD_2 - 24 hours - calculated500 mg. PuO_2 - 24 hours - calculatedFigure 2. Neutron diffraction data for CaF_2 (top) and predicted room-temperature data for $\text{AmD}_{2.6}$ (middle) and PuO_2 (bottom).

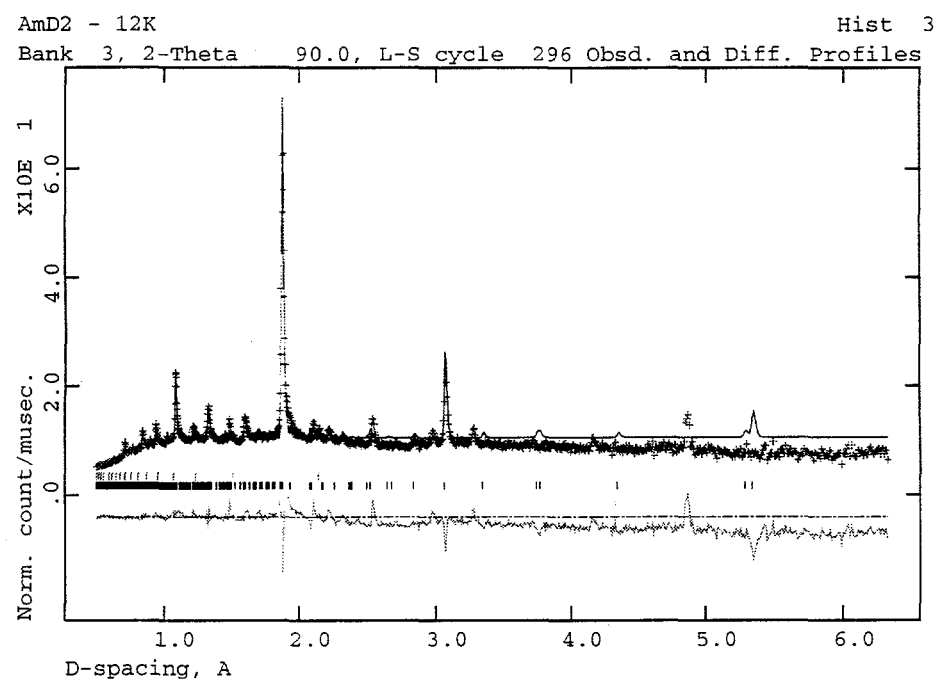


Figure 3. Neutron diffraction pattern from a 200-mg sample of $\text{AmD}_{2,4}$. The vertical lines indicate peak positions, and the lower curve indicates deviations from the fit to the data.

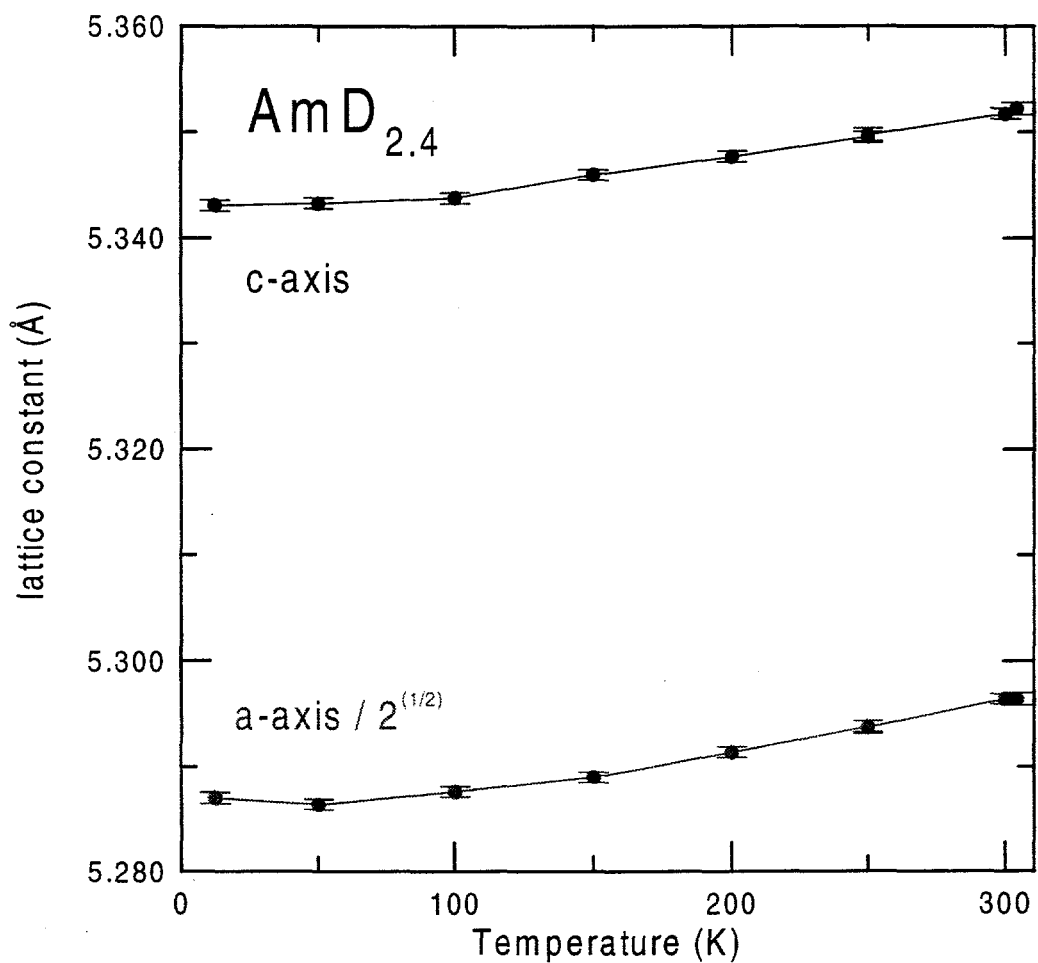


Figure 4. Lattice constants versus temperature for AmD_{2.4}.

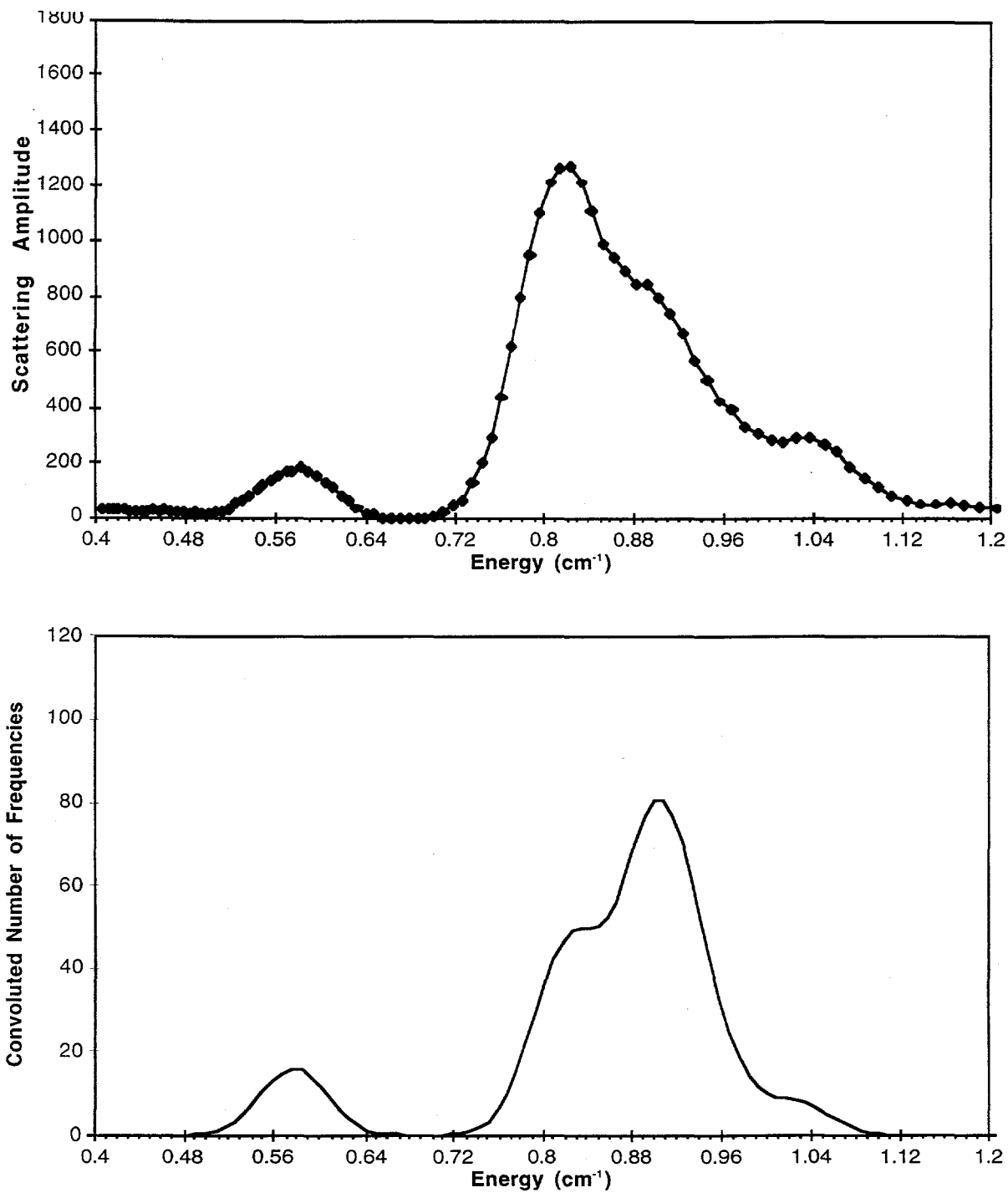


Figure 5. The spectra for CeH_{2.09} show the quality of agreement between the experimental data (top) and the lattice dynamics model (bottom).

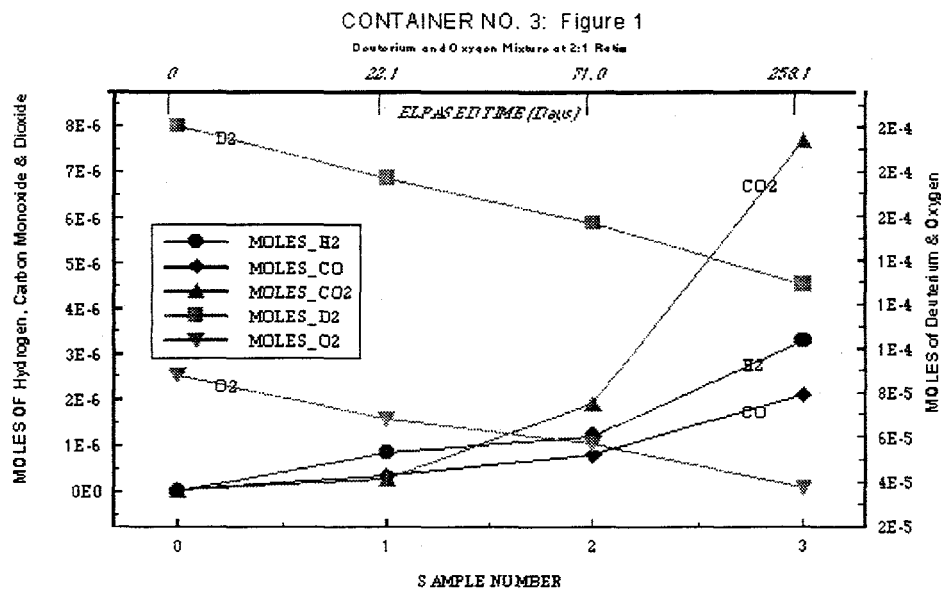


Figure 6. The data for the reaction of PuO_2 with a 2:1 ratio of deuterium and oxygen shows that the consumption of deuterium and oxygen over time forms the gaseous reaction products CO_2 , H_2 , and CO . The consumption resulting in gas products does not account for the total drop in oxygen pressure, which indicates that higher plutonium oxides are also formed.

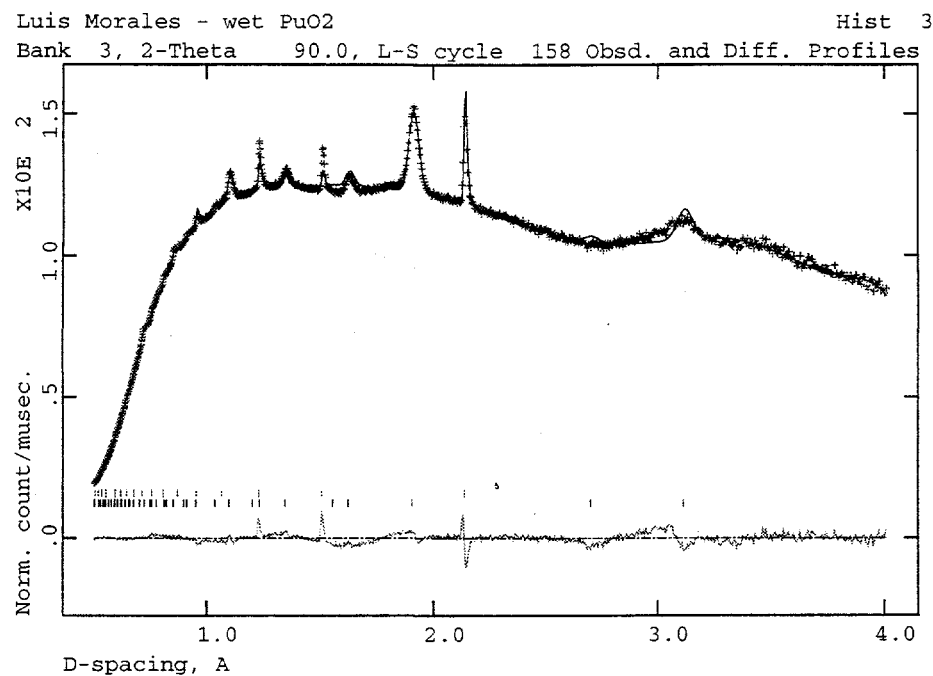


Figure 7. Neutron diffraction data for PuO_2 , including peaks for vanadium. The vertical lines indicate peak positions, and the lower curve indicates deviations from the fit to the data.